Journal of Receptors and Signal Transduction

ISSN: 1079-9893 (Print) 1532-4281 (Online) Journal homepage: http://www.tandfonline.com/loi/irst20

A novel PDE1A coupled to M_2AChR at plasma membranes from bovine tracheal smooth muscle

Patrizzia Mastromatteo-Alberga, Fabiola Placeres-Uray, Marcelo A. Alfonzo-González, Ramona Gonzalez de Alfonzo, Itala Lippo de Becemberg & Marcelo J. Alfonzo

To cite this article: Patrizzia Mastromatteo-Alberga, Fabiola Placeres-Uray, Marcelo A. Alfonzo-González, Ramona Gonzalez de Alfonzo, Itala Lippo de Becemberg & Marcelo J. Alfonzo (2015): A novel PDE1A coupled to M_2AChR at plasma membranes from bovine tracheal smooth muscle, Journal of Receptors and Signal Transduction, DOI: 10.3109/10799893.2015.1101136

To link to this article: http://dx.doi.org/10.3109/10799893.2015.1101136

Published online: 29 Oct 2015.

Journal of Receptors and Signal Transduction

http://informahealthcare.com/rst
ISSN: 1079-9893 (print), 1532-4281 (electronic)

J Recept Signal Transduct, Early Online: 1–10
 DOI: 10.3109/10799893.2015.1101136

Taylor & Francis
Taylor & Francis Group

RESEARCH ARTICLE

A novel PDE1A coupled to M_2AChR at plasma membranes from bovine tracheal smooth muscle

Patrizzia Mastromatteo-Alberga, Fabiola Placeres-Uray, Marcelo A. Alfonzo-González, Ramona Gonzalez de Alfonzo, Itala Lippo de Becemberg, and Marcelo J. Alfonzo

Sección de Biomembranas, Facultad de Medicina, Universidad Central de Venezuela, Instituto de Medicina Experimental, Caracas, Venezuela

Abstract

Muscarinic antagonists, via muscarinic receptors increase the cAMP/cGMP levels at bovine tracheal smooth muscle (BTSM) through the inhibition of phosphodiesterases (PDEs), displaying a similar behavior of vinpocetine (a specific-PDE1 inhibitor). The presence of PDE1 hydrolyzing both cyclic nucleotides in BTSM strips was revealed. Moreover, a vinpocetine and muscarinic antagonists inhibited PDE1 located at plasma membranes (PM) fractions from BTSM showing such inhibition, an M_2AChR pharmacological profile. Therefore, a novel Ca^{2+}/CaM dependent and vinpocetine inhibited PDE1 was purified and characterized at PM fractions from BTSM. This PDE1 activity was removed from PM fractions using a hypotonic buffer and purified some 38 fold using two columns (Q-Sepharose and CaM-agarose). This PDE1 was stimulated by CaM and inhibited by vinpocetine showing two bands in PAGE-SDS (56, 58 kDa) being the 58 kDa identified as PDE1A by Western blotts. This PDE1A activity was assayed with [^{3}H]cGMP and [^{3}H]cAMP exhibiting a higher affinity as K_m (μM) for cGMP than cAMP but being close values with V_{max} cAMP/cGMP ratio of 1.5. The co-factor Mg^{2+} showed similar $K_{(A)}$ (mM) for both cyclic nucleotides. Vinpocetine showed similar inhibition concentration 50% (IC_{50} of 4.9 and 4.6 μM) for cAMP and cGMP, respectively. CaM stimulated the cyclic nucleotides hydrolysis by PDE1A exhibiting similar activation constant as $K_{(CaM)}$, in nM range. The original finding was the identification and purification of a vinpocetine and muscarinic antagonist-inhibited and CaM-activated PM-bound PDE1A, linked to M_2AChR. A model of this novel signal transducing cascade for the regulation of cyclic nucleotides levels at BTSM is proposed.

Keywords

Airway smooth muscle, asthma, m2AChR, muscarinic antagonists

History

Received 1 August 2015
Accepted 7 September 2015
Published online 27 October 2015

Abbreviations: ASM: Airway smooth muscle; **BTSM**: Bovine Tracheal Smooth Muscle; **Benzamidine**: amidinobenzene hydrochloride; **CaM**: calmodulin; **CCh**: carbamylcholine; **cAMP**: cyclic adenosine 3′, 5′-monophosphate; **cGMP**: cyclic guanosine 3′,5′- monophosphate; **4-DAMP**: 4-diphenylacetoxy-N-methylpiperidine; **DTT**: 1:4-dithiothreitol; **PDE1A**: phosphodiesterase 1A; **PDE1B**: phosphodiesterase tipo 1B; **PDE1C**: phosphodiesterase tipo 1C; **PMSF**: phenylmethylsulphonylfluoride; **IBMX**: isobutyl-methylxanthine; GPCR: G protein-coupled receptors; **mAchR or MAchR**: muscarinic acetylcholine receptor; **M_2AChR**: M_2 muscarinic receptor; M_3AChR: M_3 muscarinic receptor; **NO-sGC**: NO sensitive soluble guanylyl cyclase; **NPR-GC**: Natriuretic Peptides Receptor guanylyl cyclase; **TCA**: Trichloroacetic acid; Vinpocetine: (3α: 16β)-eburnamenine-14-carboxylic ethyl ester acid

Introduction

Muscarinic activation of Airway smooth muscle (ASM) is relevant in the broncho-constriction presents in asthma (1–3). Acetylcholine acting on muscarinic receptors (MAChRs) at the ASM sarcolemma stimulate signal transducing cascades to activate the ASM machinery (3,4). The MAChRs belong to the GPCR family linked to intracellular specific effectors (5,6). Mammalian MAChRs (m_1-m_5) have been described (6) and ASM expresses both m_2 and m_3AChRs (7). ASM has a mixed population of M_2 and M_3AChRs (8) being the M_2AChRs more abundant at plasma membranes (PM) fractions from ASM (9,10). MAChRs are involved in the rise/decline of cAMP/cGMP levels in ASM. Thus, atropine (a non-selective muscarinic antagonist), significantly increased the cGMP and cAMP levels at bovine tracheal smooth muscle (BTSM) being this effect similar to the ones produced by vinpocetine, a specific PDE1 inhibitor (11). Consequently, muscarinic antagonists and vinpocetine effects may be the result of the PDE1 inhibition (12). Tracheal smooth muscle

Address for correspondence: Marcelo J. Alfonzo, Sección de Biomembranas, Facultad de Medicina, Instituto de Medicina Experimental, Universidad Central de Venezuela, Sabana Grande 50587, Caracas, Venezuela. E-mail: hmag5@hotmail.com

(TSM) exhibits Ca^{2+}/CaM-dependent PDE1s (CaM-PDE) that hydrolyzes cAMP and cGMP with equal capacity (13–15). CaM-PDEs are mediators between the Ca^{2+} and cyclic nucleotides second messenger allowing cyclic nucleotide-dependent processes to be regulated by $[Ca^{2+}]_i$ (16). PDE1 family has three genes (PDE1A, PDE1B and PDE1C) (17).

In this work, the functional presence of PDE1 at BTSM strips was demonstrated. Moreover, a PM-bound PDE1 was purified, characterized as a vinpocetine-inhibited and CaM-stimulated PDE activity with MW of 58 kDa and identified by Western blotting as PDE1A. Moreover, a novel signal-transducing cascade linking an M_2AChR to this membrane-bound PDE1A is proposed.

Methods

The compounds from Sigma-Aldrich (St. Louis, MO, U.S.A) : Trizma Base, PMSF, DTT, sucrose, benzamidine, EGTA, EDTA, cAMP, cGMP, Q-sepharose, CaM-agarose, HEPES, atropine, 4-DAMP, vinpocetine and snake venon 5′ nucleotidase. Kits for cGMP determination (TRK-500) and ECL Western Blotting Reagent Pack from GE/Healthcare, Life Sciences (Little Chalfont, United Kingdom). Kits for cAMP Radioassay determination (KAPH2-172) from Diagnostic Products Corporation (Los Angeles, CA, U.S.A.) . Cyclic [8,5-^{3}H] GMP (25–50 Ci/mmol) and cyclic [5′,8-^{3}H] AMP (30–60 Ci/mmol), from Perkin Elmer (Waltham, MA, U.S.A) . Reagents for SDS-PAGE and protein (Mw) standards, Dowex-1-X-8 (chloride form) and Precision Plus protein™ (BIORAD, Hercules, CA, U.S.A.) Western C ™ (BIORAD, Hercules, CA, U.S.A.) Pack from BIORAD (USA). Other chemicals pro-analysis grade from E. Merck (Darmstadt, Germany) and Fisher (Waltham, MA, U.S.A). The recombinant CaM was produced using bacteria *E. coli* strain BL21 (DE3) pLysS transformed with plasmid pETCM under the control of a T7 promoter. Antibodies from Santa Cruz Biotechnology (Santa Cruz, CA, U.S.A.), as polyclonal IgG: human origin PDE1A, polyclonal IgG of PDE1B of human origin and Polyclonal IgG of PDE1C of human origin.

Preparation and incubation of bovine TSM strips

Bovine tracheas obtained from a local slaughterhouse were processed as described (18). To evaluate the cAMP/cGMP content, BTSM strips were placed into a specially designed multi-organ chamber (400 mL) with 95% O_2 and 5% CO_2, holding simultaneously several BTSM strips at 37 °C, at 1 g of tension. BTSM strips were removed at specific times and placed into liquid nitrogen.

Measurement of cyclic nucleotides in bovine TSM strips

Frozen BTSM strips were homogenized in 5% TCA (18). TCA extractions were performed twice, and the insoluble material was removed by centrifugation at $1500 \times g$ for 10 min at 4 °C, which was processed for protein determination and the acid supernatants were combined, extracted twice with ether to remove TCA, frozen at –80 °C and lyophilized (18). The acid-soluble nucleotide extract was dissolved in a small volume of 50 mM Tris-HCl, 4 mM EDTA, pH 7.4, and kept frozen at −80 °C. The cyclic nucleotide recovery was between 95 and 98% for both nucleotides. Cyclic GMP was determined using a radioimmunoassay with a commercial kit (TRK-500) (19). Cyclic AMP was determined using a radioassay kit (KAPH2-172) as described (20).

Subcellular fractionation and plasma membranes preparation from BTSM

The subcellular fractionation of BTSM and the isolation of the plasma membrane fractions (PM) were performed as described (20). This procedure was slightly modified to improve the yield of PM fraction. Thus, in the original procedure, there is a discontinuous sucrose gradient assembled by the 0.3 M/0.82 M/1.28 M sucrose solutions. The 0.82 M sucrose was removed and the PM fraction was collected at 0.3 M/1.28 sucrose interphase.

The extraction of vinpocetine-inhibited and CaM-stimulated PDEs from plasma membrane fractions

PDE1 was extracted from PM-BTSM using a method described for membrane-bound retinal PDE6 (21). The PM fraction was incubated with a hypotonic buffer (10 mM HEPES; pH 7.0; 0.1 mM EDTA; 1 mM DTT; 0.25 mM PMSF) on ice under agitation for 15 min and centrifuged at $150\,000 \times g$ for 15 min. This extraction procedure was performed six times. All supernatants were pooled as the hypotonic extract (HE), concentrated under low speed centrifugation using Millipore YM-10 to 1–2 mL and the sediment (SED) was discarded.

The purification of vinpocetine-inhibited and CaM-stimulated PDE1 activity

The vinpocetine-inhibited and CaM-stimulated PDE1 activity was purified at 4 °C (22). Thus, an ion exchange chromatography (Q-sepharose) followed by CaM-agarose. The Q-sepharose (1×5 cm) column was equilibrated with Buffer 1 (20 mM Tris-HCl; 1 mM imidazole, 0.1 mM EGTA, 1 mM magnesium acetate) at pH 7.0 plus 5 mM DTT. Subsequently, HE was applied to Q-sepharose column, washed with 20 mL Buffer 1 containing 50 mM NaCl. Finally, the Q-column was eluted using a linear gradient of NaCl (0.4–1.0 M). Protein fractions (Pool I) and the vinpocetine-inhibited and CaM-activated PDE were evaluated.

CaM-agarose (5 mL) was washed with Buffer 1 containing 2 M Guanidine hydrochloride (23). This CaM-agarose was equilibrated with Buffer 1 containing 100 μM $CaCl_2$ and 5 mM DTT. Subsequently, ''Pool I'' was mixed with CaM-agarose and incubated overnight. The next day, the slurry was packed into a column and washed with Buffer 1. Later, CaM-agarose column eluted with Buffer 1 containing 2 mM EGTA. Protein fractions (Pool II), concentrated to 0.5–1 ml using low speed centrifugation with Millipore YM-10 and 30% ethylene glycol was added and kept at −80 °C. The vinpocetine inhibited and CaM activated PDE were evaluated in Pool II.

Cyclic nucleotide phosphodiesterase (PDE) activities

The PDE were assayed using [^{3}H]cGMP and [^{3}H]cAMP (12). Briefly, protein (10–50 μg) were incubated for 15 min at 30 °C

with (0.1 μC/assay) of either 2,8 [^{3}H]cAMP or 8-[^{3}H]cGMP in a buffer containing 0.3 mM of cAMP or cGMP, 40 mM Tris-HCl pH 7.5, 10 mM $MgCl_2$ and 1 unit of snake venon 5′ nucleotidase. Reactions were stopped with 10 mM EDTA and transfer to 4 °C. Later, samples were applied to anion exchange (AG-1-X8, Cl^- form, 200–400 mesh) (2 ml) columns and the non-charged products ([^{3}H]guanosine or [^{3}H]adenosine) eluted with 50% ethanol and transferred to vials containing Aquasol. The [^{3}H] was counted with 30% efficiency in RackBeta LKB, Wallac 1214/1219.

SDS-PAGE analysis and immunodetection of PDE isoenzymes by Western blots

PM polypeptides were separated on SDS-PAGE 10 % (24). For the Western blots, these SDS-PAGE gels were transferred to PDVF (25). Protein Blots were blocked for 2–4 hours at 4 °C in PBS-2% BSA-0.05 % (v/v) Tween 20. After washing twice with PBS-Tween, the PDVF membrane was incubated for 4–6 hours at 4° with (1/1000) polyclonal IgG specific for PDE1 (A, B, C). Then, the PDVF membrane was washed overnight with PBS-Tween 20 and incubated for 4–6 hours at 4 °C with (1/1000) HRP anti rabbit IgG. To identify the immunoreactivity proteins (positive bands), a Precision Plus protein™ Western C™ Pack and ECL Western Blotting Reagent Pack were employed.

Other procedures and methods

Protein was quantified using BSA as standard as described (26). The enzyme kinetic parameters were estimated using the program GraphPad Prism (La Jolla, CA, U.S.A.) (version 6), which requires at least three different experimental data, to obtain the kinetic enzyme parameters (K_m, V_{max}). The statistical significance was estimated using the Student *t*-test.

Results

An active PDE1 is revealed in intact BTSM strips

The existence of an active dual PDE1 in BTSM was established. BTSM strips were exposed to atropine for 15 min to raise the cAMP/cGMP levels (12). Later, they were contracted using a classic KCl (60 mM) depolarizing procedure (27) and the cAMP and cGMP content was determined. Figure 1 shows the cAMP amounts at ''0T'' was 26.1 ± 1.6 pmoles/mg protein, which sharply decreased to 6.0 ± 0.7 pmoles/mg protein at 20 s, which is similar to the cAMP level in unstimulated strips. Identical behavior was found for the cGMP levels decreasing from ''0T'' of 12.6 ± 1.5 pmoles/mg protein to basal values of 2.0 ± 0.4 pmoles/mg protein at 20 s, after KCl exposure.

Subcellular localization of vinpocetine-inhibited PDE1 (ViPDE) at BTSM

Muscarinic antagonist and vinpocetine-inhibited PDE1 (ViPDE1) are located in particulate fractions of BTSM (12). The atropine sensitive PDE was useless because this activity has poor reproducible but the ViPDE1 exhibited good reproducibility and reliable activity. Thus, BTSM subcellular fractionation (20,28) was employed to locate this ViPDE1. These fractions are: Crude extract: E, Nuclear fraction: N, Mitochondrial fraction: M, microsomal fraction: P and soluble or cytosol fraction: S. Moreover, a modification to generate the PM fraction from BTSM at the 0.3/1.28 M sucrose interface was done. All subcellular fractions were assayed using cAMP and cGMP. Table 1 shows that the crude M and P fractions displayed greater enzyme activities than the N fraction and fraction S. Moreover, the greater specific activity for both

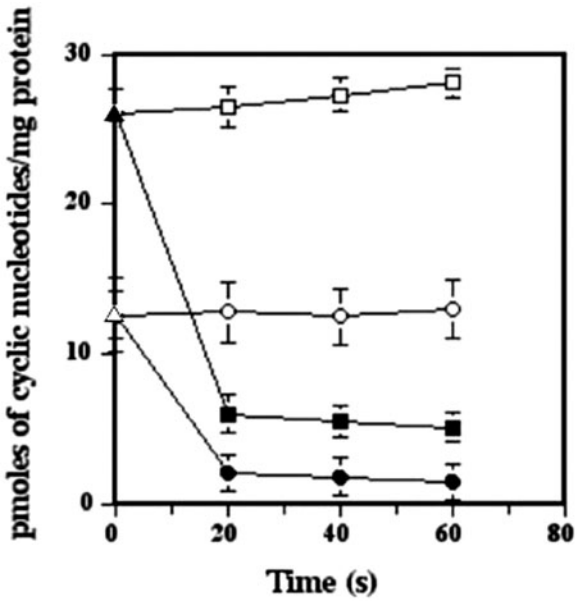

Figure 1. The time course of cyclic nucleotides levels at BTSM strips during KCl-induced contraction. Several BTSM strips (10 × 2 mm) were placed into a specially designed multi-organ chamber (400 mL) of KRB at 37 °C as described in ''Methods'' section. These BTSM strips were equilibrated during 30 min. Later, atropine (1×10^{-5} M) was added. After 15 min, KCl concentration was rise to 60 mM to induce BTSM depolarization. Each 20 s, individual strips were removed and placed into liquid nitrogen and the cyclic nucleotide extraction and determination were performed as described in Methods. Each value is the mean ± SE of 5 different BTSM strips. Basal cGMP at 0T (Δ); Basal cAMP 0T (▲), Basal cGMP (○); Basal cAMP (□); cGMP plus KCl (●); cAMP plus KCl (■).

Table 1. Subcellular location of the vinpocetine-inhibited PDE1 (ViPDE).

Fractions	cAMP	cGMP
E	4.51 ± 0.22	4.02 ± 0.43
N	1.53 ± 0.15	1.50 ± 0.18
M	4.58 ± 0.27	4.17 ± 0.10
S	1.21 ± 0.14	1.02 ± 0.11
P	5.24 ± 0.23	5.02 ± 0.18
PM	7.89 ± 0.42	7.12 ± 0.31

The vinpocetine-inhibited PDE1 (ViPDE) as pmoles of cyclic nucleotides hydrolyzed/min/mg protein was evaluated during the subcellular fractionation procedure, which was estimated as the Basal PDE activity minus the PDE activity in the presence of vinpocetine. The enzyme activity was determined using [^{3}H]cGMP and [^{3}H]cAMP as substrates in the presence or absence of 20 μM vinpocetine as described in Methods. The samples evaluated were: E: crude extract, N: Nuclear fraction, S: Cytosol, P: Microsomal fraction and PM: plasma membranes fraction. Data are the mean ± SE of ViPDE activity assayed in duplicate from five (5) different subcellular preparations of BTSM.

cAMP and cGMP was found at PM fraction in comparison to other subcellular fractions. These results indicated that the ViPDE1 is associated with the PM fractions.

Muscarinic M_2AChR regulate the PM-bound ViPDE1

PM fractions from BTSM exhibit high concentrations of M_2AChR subtype (10). Thus, classic M_3AChR muscarinic antagonist, such as 4-DAMP and methoctramine as an M_2AChR-selective antagonist were assayed. In Figure 2, methoctramine was more potent than 4-DAMP to inhibit this PM-bound-PDE1 showing methoctramine, an $IC_{50} = -8.12 \pm 0.21$ and 4-DAMP, an $IC_{50} = -6.68 \pm 0.13$. These results suggest that a pharmacological profile of an M_2AChR (10) is responsible of PDE1 inhibition.

Extraction of ViPDE1 from PM fractions

Membrane proteins as PDE1 can be extracted/solubilized using procedures such as high/low ionic strength treatments or detergents. Initially, low/high ionic buffers were tested and the low ionic strength buffer was the best procedure to remove most of the ViPDE. Thus, the ViPDE was removed using a similar procedure for the extraction of membrane-bound cGMP-PDE6 from the bovine retinal cones (21). Thus a hypotonic buffer containing 10 mM HEPES, 0.1 mM EDTA, 1 mM DTT and 0.25 mM PMSF at pH 7.5 was employed. Table 2 indicates that most of the ViPDE was at the hypotonic extract (HE), whereas, a low ViPDE was at the sediment remnants (SED) and the atropine sensitive PDE was absent in the HE fraction. This was the reason that the vinpocetine inhibition (ViPDE) activity was the main tool for the PDE1 purification.

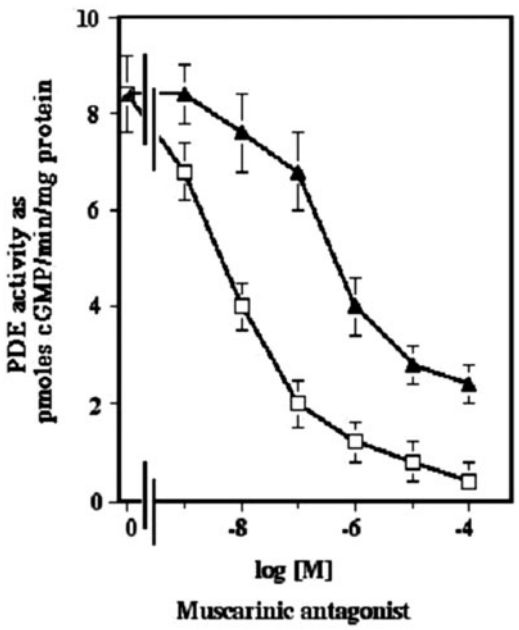

Figure 2. Effect of muscarinic antagonists on the PDE1 activity at plasma membranes fraction from BTSM. PM-BTSM (20–30 μg) fractions were incubated with [3H] cGMP as PDE substrate as described in ''Methods'' section. A dose titration curve of muscarinic antagonists such as methoctramine (□) and 4-DAMP (▲) were performed. The inhibitory concentration IC50 was estimated as described in Methods. Data are the mean ± SE of three (3) different PM preparations.

Purification of the ViPDE using Q-sepharose and CaM-agarose columns.

The ViPDE1 activity was purified as described (22) and modified. The EH was applied to Q-sepharose column, equilibrated with buffer 1. Later, the Q-sepharose was washed with of buffer 1 containing 50 mM NaCl. Finally, the Q-sepharose was eluted with a linear gradient of NaCl (0.4–1.0 M) as shown in Figure 3(A). ''Pool I'' protein was concentrated to 1.0 to 2.0 mL using a Millipore YM-10. The inset of Figure 3(A) shows that PDE1 was inhibited in about 70% by vinpocetine (20 μM vinpocetine), while CaM (5 nM) increased in more than 80% this PDE1.

Purification of the ViPDE1 using a CaM affinity column.

PDE1 possess two CaM binding sites, which allowed the purification of this PDE1 using a CaM agarose. This affinity column was washed with 2 M Guanidine-HCl and equilibrated with Buffer 1 containing 100 μM Ca^{2+} and 5 mM DTT. Subsequently, ''Pool I'' was mixed with CaM agarose and incubated overnight at 4 °C. The next day, the column was packed and washed with Buffer 1 (without Ca^{2+} or EGTA), eluted with Buffer 1 containing 2 mM EGTA as shown in Figure 3(B). Protein fractions as ''Pool II'' were concentrated using a Millipore YM-10 (Billerica, MA, USA), up to 1–2 mL and, ethylene glycol was added 30% and stored at −80 °C. The inset of Figure 3B shows that vinpocetine (20 μM) inhibited significantly in 70%. However, CaM (5 nM) increased at more than double (116%) of PDE.

A summary of the purification of the ViPDE1 is shown in Table 3. E fraction showed a specific activity of 4.0 ± 0.2 pmoles/min/mg protein to the Pool II from CaM-agarose with of 152 ± 8 pmoles/min/mg protein, rendering purification around 38 times. PDE1 activity in ''Pool I'' exhibits specific activity of 72 ± 6 pmoles/min/mg protein, being some 18 times of purification, which was the enzyme sample used to perform the kinetic enzyme characterization.

Determination of K_m and V_{max} for cAMP and cGMP, the $K_{(A)}$ for Mg^{2+}, the $K_{(CaM)}$ for CaM and IC_{50} for vinpocetine of the ViPDE1

The kinetic parameters were determined using the partially purified PDE1 presents in ''Pool I'', being more stable

Table 2. Evaluation of the ViPDE and atropine sensitive activities during the hypotonic extraction of PM from BTSM.

Fractions	ViPDE activity	Atropine sensitive PDE
PM	7.16 ± 1.22	8.12 ± 1.87
HE	15.32 ± 0.22	1.02 ± 0.18
SED	1.58 ± 0.29	1.24 ± 0.21

The vinpocetine-inhibited PDE1 (ViPDE) and atropine-sensitive PDE were evaluated during the extraction procedure. The ViPDE and atropine sensitive PDE were estimated as the Basal PDE activity minus the PDE activity in the presence of either 20 μM vinpocetine or 1 μM atropine. The enzyme activity was determined using [^{3}H]cGMP as substrate as described in Methods section. The samples evaluated were: PM: plasma membranes fraction, HE: Hypotonic extract, SED: Sediment. Data are the mean ± SE of PDE activity assayed in duplicate from five (5) different PM extraction preparations.

activity and abundant protein. Initially, the proportionality between the protein concentration and PDE1 activity was established being linear to 50 µg protein. Figure 4(A) shows the kinetic behavior in the presence of cAMP/cGMP on the PDE1. Thus, both cyclic nucleotides increased the PDE1 activity, in a concentration dependent manner, reaching saturation at 20 µM or greater for both nucleotides. The K_m for cAMP (8.4 ± 0.7 µM) versus K_m for cGMP (6.1 ± 1.5 µM) showing more affinity for cGMP. Additionally, the V_{max} for cAMP (99 ± 3 pmoles/min/mg protein) was significantly higher ($p < 0.05$) than V_{max} for cGMP (66 ± 5 pmoles/min/mg of protein) displaying a cAMP/cGMP V_{max} ratio of 1.5.

The Mg^{2+} dependency of the PDE1, in presence of cAMP and cGMP was studied. Figure 4(B) shows that increasing concentrations of Mg^{2+} augmented the PDE1 activity reaching maximal response at 1 mM Mg^{2+} for both cyclic nucleotides. Likewise, the $K_{(A)}$ for Mg^{2+} were determined in the presence of cAMP (0.32 ± 0.02 mM) and in the presence of cGMP a $K_{(A)}$ of 0.24 ± 0.01 mM. These $K_{(A)}$ parameters exhibited close values for both cyclic nucleotides. The inhibitory effect of vinpocetine was evaluated in Figure 5(A), increasing amounts of this inhibitor decreased PDE1. Thus, the $IC_{50} = 4.9 \pm 0.2$ µM for vinpocetine in the presence of the cAMP and an $IC_{50} = 4.6 \pm 0.3$ µM with cGMP were estimated. Thus, a similar kinetic behavior towards vinpocetine, independently of the cyclic nucleotides was observed. A classic biochemical property of the PDE1 family is the CaM stimulation. Figure 5(B) shows an increment of

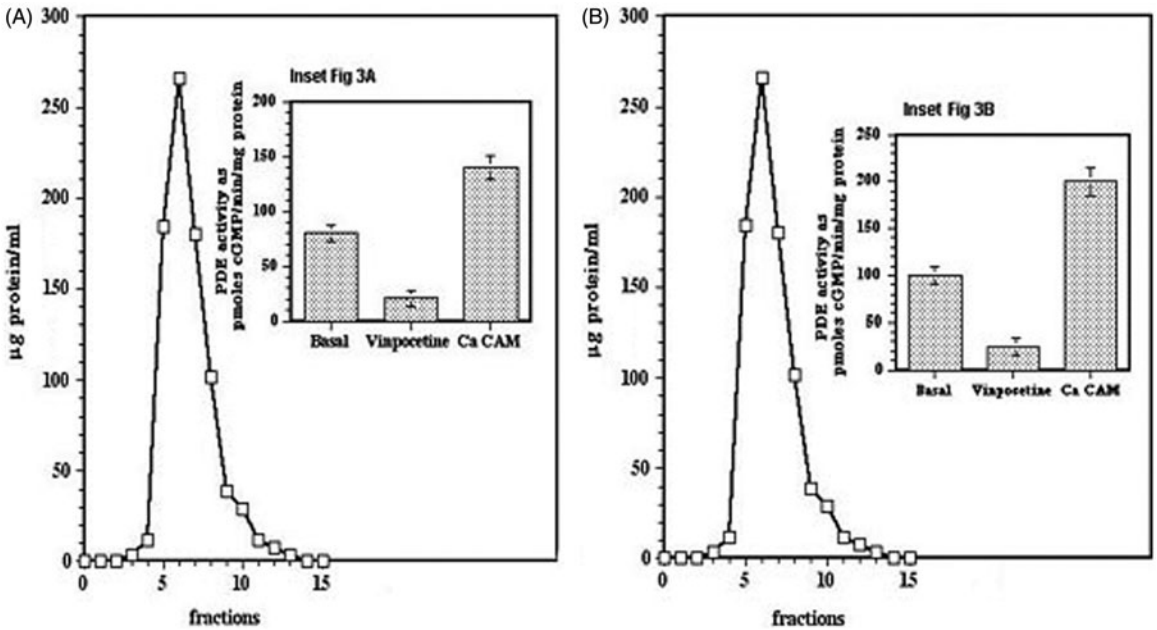

Figure 3. (A) Typical protein elution profile from Q-sepharose column. HE was applied to a Q-sepharose and washed with buffer 1 plus 50 mM NaCl and eluted with a linear gradient of NaCl (0.4 – 1.0 M) as shown. Protein fractions were grouped as ''Pool I''. Inset: The vinpocetine and CaM effects on the PDE activity assayed at ''Pool I''(20–30 µg protein) and [3H] cGMP with Ca2+/CaM (1 mM/5 nM) and Vinpocetine (20 µM). Data are the mean ± SE of five preparations assayed by duplicate. *$p < 0.05$; Basal PDE1 versus Ca2+/CaMPDE1. **$p < 0.001$; Basal PDE1 versus ViPDE1. (B) Typical protein profile from (CaM-agarose) affinity column. The Pool-I was placed on CaM-agarose equilibrated with buffer 1 plus 100 µM Ca2+ and 5 mM DTT and incubated overnight at 4 °C. Later, the column was washed with buffer 1 without Ca2+ or EGTA. Later, the CaM-agarose was eluted with buffer 1 containing 2 mM EGTA and protein fractions were grouped into a ''Pool II'', concentrated using a Millipore YM-10. Inset.- The inhibitory effect of Vinpocetine and stimulation by CaM at ''Pool II''. The PDE activity was determined using ''Pool II'' (10–20 µg protein) and [3H]cGMP with Ca2+/CaM (1 mM/5 nM) and Vinpocetine (20 µM) Data are the mean ± SE of five (5) preparations assayed in duplicate. *$p < 0.05$; Basal PDE versus Ca2+/CaMPDE. **$p < 0.001$; Basal PDE versus ViPDE1.

Table 3. Purification and activity of the vinpocetine-inhibited PDE1 from bovine tracheal smooth muscle.

Fractions	Protein (mg/mL)	Vol (mL)	Total Protein (mg)	S.A. pmol/min/mg	Total Activity (pmol/min)	Purification Factor
E	10.2 ± 0.22	900	$9{,}180 \pm 198$	4.0 ± 0.2	$36{,}720 \pm 790$	1.0
PM	7.0 ± 0.15	50	350 ± 18	7.2 ± 0.3	$2{,}520 \pm 120$	1.8
HE	0.18 ± 0.02	900	162 ± 10	14.1 ± 0.4	$2{,}268 \pm 90$	3.5
Pool I	5.2 ± 0.4	2.0	10.4 ± 0.8	72.1 ± 6.2	750 ± 40	18.0
Pool II	1.0 ± 0.1	0.5	0.5 ± 0.04	152.1 ± 8.2	76 ± 4	38.0

The vinpocetine-inhibited PDE1 (ViPDE) activity was evaluated during the purification procedure. ViPDE was estimated as the subtraction of Basal PDE activity minus the PDE activity in the presence of vinpocetine. Protein content was measured as described in Methods. The enzyme activity was determined using [^{3}H]cGMP as substrate in the presence or absence of 20 µM vinpocetine as described in Methods. The samples evaluated were: E: crude extract, PM: plasma membranes fraction, HE: hypotonic extract, Pool I: Active fractions obtained from Q-sepharose column, Pool II: Active fractions from CaM-agarose column. The purification factor was estimated as the ratio of the specific activity (S.A.) of each fraction divided into the specific activity of E fraction. Data are the mean ± SE of ViPDE activity assayed in duplicate from five (5) different subcellular preparations of BTSM.

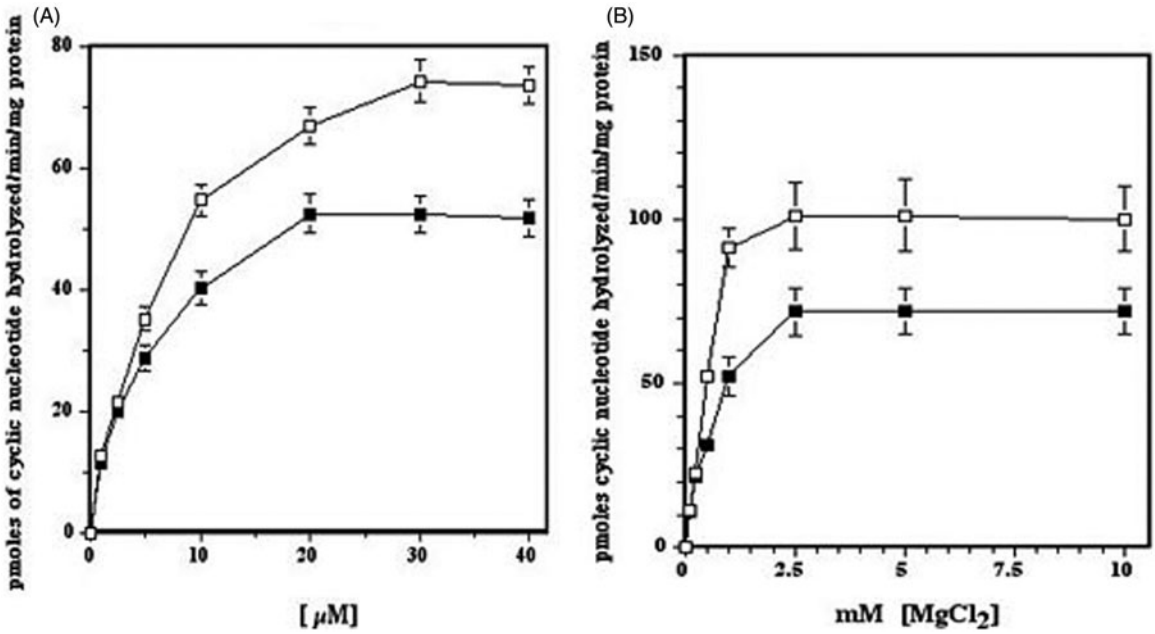

Figure 4. (A) Kinetic behavior of PDE1A in the presence of cAMP/cGMP. The ''Pool-I'' (30–40 μg of protein) was incubated at 30 °C for 15 min, and increasing concentrations of cAMP(□)/cGMP (■) as described in the ''Methods'' section. The PDE 1 activity was expressed as pmoles of cyclic nucleotide hydrolyzed/min/mg protein. The K_m and V_{max} were determined as described in Methods. Data represent the mean ± SE of three (3) different preparations. (B) The magnesium (MgCl2) titration on the PDE1A activity. The ''Pool-I'' (30–40 μg of protein) was incubated with increasing concentrations of MgCl2 in the presence of cAMP(□)/cGMP (■)as described in Methods section. The kinetic parameters ($K(A)$ and V_{max}) were determined as described in the ''Methods'' section. Data represent the mean ± SE of three (3) different preparations.

Figure 5. (A) Kinetic behavior of PDE1A in the presence of Vinpocetine. The ''Pool-I'' (30–40 μg of protein) was incubated with increasing doses of vinpocetine in the presence of cAMP(□)/cGMP (■) as described in the ''Methods'' section. The K_m and V_{max} were determined as described in Methods. Data represent the mean ± SE of three (3) different preparations. (B) The effect of calmodulin on the PDE1A activity. The ''Pool-I'' section (30–40 μg of protein) was incubated with increasing amounts of CaM in the presence of cAMP(□)/cGMP (■) as described in the ''Methods'' section. The kinetic parameters (K_m and V_{max}) were determined as described in Methods section. Data represent the mean ± SE of three (3) different preparations.

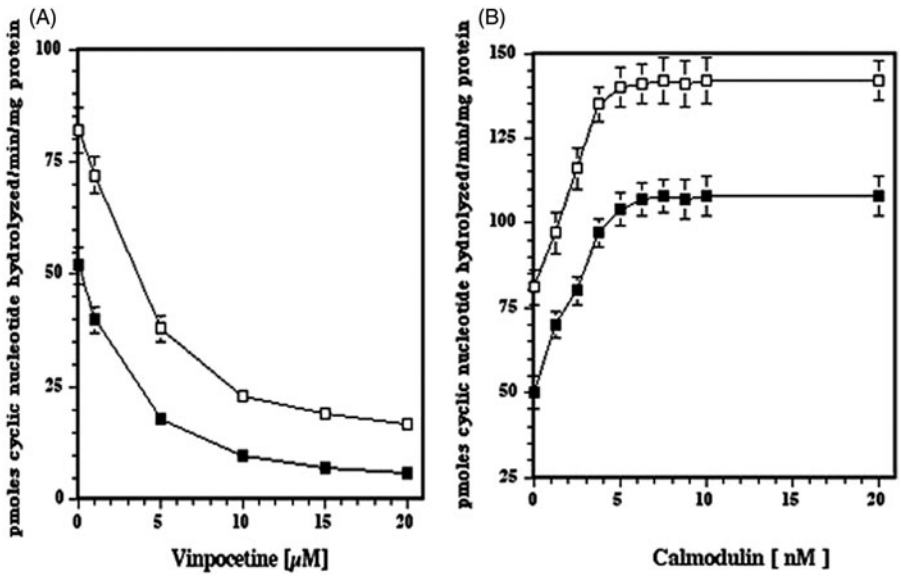

PDE1 activity as CaM increased, reaching a maximal response at 5 nM CaM. Accordingly, the CaM concentration required for half-maximal activation ($K_{(CaM)}$); in the presence of the cAMP was 2.0 ± 0.5 nM, while with cGMP was 1.6 ± 0.3 nM. These data indicate similar CaM activation being independent of cyclic nucleotides used.

SDS-PAGE analysis of the ViPDE active fractions

SDS-PAGE 10% was performed as shown in Figure 6. Thus the PM fraction (lane 1) and HE (lane 2) displayed similar dense membrane polypeptides pattern. The Pool I from Q-sepharose (lane 3), the protein bands decreased significantly to a define pattern. Finally, CaM-agarose (lane 4) renders a greatest purification showing two relevant bands of 56 and 58 kDa. An Mw protein standard from 28.3 to 132 kDa is shown in line 5.

Identification of PDE1A by Western-blotting analysis.

Western-blotts using specific antibodies against PDE1A, PDE1B and PDE1C isoforms were employed to identify this Vi-PDE1. SDS-PAGE 10% gels were transferred to the PDVF membranes being exposed to the antibodies against the

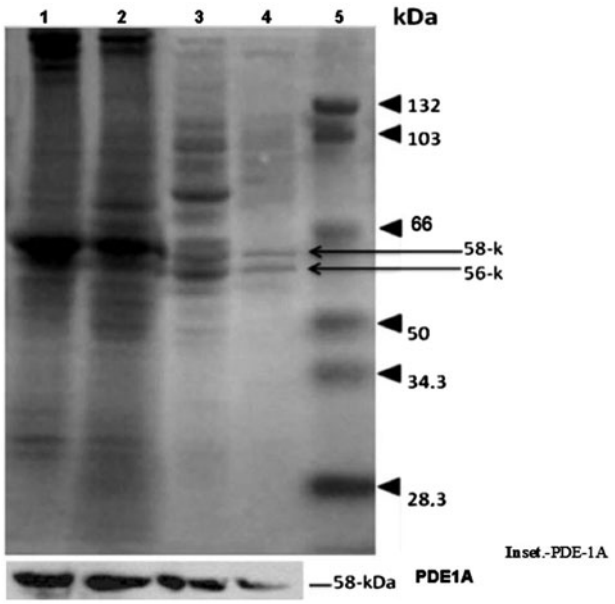

Figure 6. SDS-PAGE and Western blotts from BTSM containing active PDE1. Membrane proteins (5–50μg) were analyzed on SDS-PAGE 10% gels. The samples were: Lane 1: PM (50 μg). Lane 2: HE (50 μg). Lane 3: ''Pool I'', (15 μg). Lane 4: ''Pool II'', (5 μg). Lane 5: Protein standards (Mw) from 28.3 to 132 kDa. Inset.-PDE-1A: Western blots for the PDE1 purified from the BTSM. Protein samples were run on SDS-PAGE 10% gels and transferred to PDVF membranes, which were incubated with specific antibodies against the PDE1A isoform as described in the ''Methods'' section. Lane 1: PM (50 μg). Lane 2: HE (50 μg). Lane 3: ''Pool I'', (15 μg). Lane 4: ''Pool II'', (5 μg).

three PDE1 isozymes. It can be seen in lower inset of Figure 6 that the anti-PDE1A antibodies detected a signal corresponding to a band, which migrated at MWapp ≈58 kDa in all samples analyzed, i.e. PM, HE, Pool I and Pool II fractions. The PDE1B and PDE1C antibodies were negative on the PDVF membranes. These Western blotts demonstrated that a PDE1A is located at PM from BTSM.

Discussion

Muscarinic antagonists and vinpocetine (PDE1 inhibitor) increased simultaneously both cAMP and cGMP levels in BTSM, via the inhibition of PDE1 (12). Several topics were addressed: (i) the demonstration of an active PDE1 in intact BTSM. (ii) the subcellular location of a ViPDE1. (iii) The muscarinic receptor subtype involves in this muscarinic antagonist inhibition. (iv) the isolation and purification of this membrane-bound ViPDE1. (v) the identification of this ViPDE1 as a PDE1A using Western-blotts. (vi) the kinetic enzymatic characterization of this PDE1A.

Atropine raises the cyclic nucleotides content in BSTM strips (12), which were contracted using the KCl depolarizing procedure (27), inducing at 20 s, a dramatic fall in the cyclic nucleotides content at BTSM strips. This decline in both cyclic nucleotides levels may be a result of CaM-PDE1 activation, via KCl induces membrane depolarization and initiates a Ca^{2+}influx, through the opening of L-type Ca^{2+} channels located at BTSM sarcolemma increasing the $[Ca^{2+}]_i$ and the active CaM levels (27) inducing the activation of the BTSM contraction machinery (29) and the PDE1s (22,30). The existence of an active PDE1 enzyme in intact BTSM was demonstrated.

The muscarinic antagonist inhibited and ViPDE1 activity was present at particulate fractions from the BTSM (12). Thus, ViPDE1 was more active in the presence of cAMP than cGMP and detected in particulate fractions such as Nuclear (N), Mitochondrial (M) and Microsomal (P) fractions with little activity at cytosol (S) fraction. Moreover, the PM fractions displayed the highest specific PDE activity.

This PDE1 was inhibited by muscarinic antagonists acting on M_2AChRs at the sarcolemma from BTSM (10,20,28). Thus, methoctramine (M_2AChR selective antagonist) (31) was more effective than 4-DAMP (a M_3AChR selective antagonist) (32) inhibiting this membrane-bound PDE1A. This pharmacological profile belongs to an M_2AChR (10). ASM displays a mixed population of M_2 and M_3 subtypes (8) being the M_2 subtype, the most abundant at PM-BTSM (10). M_2AChRs participate directly in ASM contraction via Gi/o proteins (18,33–37). However, our experimental data provided by the muscarinic-antagonists inhibition of ViPDE1A at PM-BTSM, took place in the absence of GTP or analogs, suggesting a direct coupling mechanism between M_2AChR and ViPDE1A. In this sense, a direct coupling mechanism has been demonstrated for other GPCR as a direct interaction between the M_3AChR, and its effector enzyme, PLC β3 (38).

The muscarinic antagonist inhibition was lost as this PDE1 was removed from the PM because the M_2AChRs remained at the sediment. Consequently, the PDE1 purification was followed using the ViPDE1 activity. This PDE1A from PM-BTSM was extracted using a hypotonic buffer, as described for the isolation of the membrane-bound PDE6 (21). PDE6 is heteromeric protein (39) and plays role in visual signal transduction by regulating cGMP levels (21,40). Furthermore, PDE6s anchor to the membranes since the catalytic subunits PDE6α and PDE6β, are post-translationally farnesylated and geranylgeranylated, respectively (41). Other PDE1 activities have identified in spermatozoa, associated with the PM (50–60%) (42). This membrane-PDE1A activity is solubilized using Triton X-100, which was not stimulated by CaM because CaM is tightly bound to this PDE1A (43). These biochemical properties of PDE1A from spermatozoa are distinctive of the PDE1A here described.

The PDE1s catalyze the degradation of cAMP and cGMP to their 5′AMP and 5′GMP and constitute a large family (44,45), with three PDE1A, B and C genes (46), which in turn give rise to multiple isoforms by alternative ''splicing'' of mRNA (17,47–49), differing in their ends (C-and N-terminal) sequence. The family of the PDE1s has a similar structure divided into three domains: A regulatory containing two CaM-binding domains located at the N-terminal end and a conserved catalytic domain and dimerization motif at C-terminal (17,46,50,51). The PDE1 isoform here characterized was identified by Western blotts using specific polyclonal antibodies against the PDE1A, PDE1B and PDE1C. Only a positive band for PDE1A with a 58 kDa was found from the PM, HE, Pool I and Pool II fractions. Other antibodies against the PDE1B and PDE1C isoforms were negative. After the CaM-agarose column, the presence of doublet relevant bands of 56–58 kDa in SDS-PAGE was observed. The 58 kDa band is PDE1A while the 56 kDa band could be protein-partner similar to that previously identified in rat spermatozoa as a CaM binding protein with still unknown function (52).

The affinity for cGMP of this PDE1A was slightly higher than cAMP. This selectivity for cGMP being lower for the cAMP has been described for PDE1A and PDE1B (50). This PDE1A is different to the PDE1C, which hydrolyzes both cyclic nucleotides with similar high affinity (50).

PDEs require Mg^{2+} for activity. This PDE1A exhibited a classic Michaelis–Menten behavior for Mg^{2+} as an activator. Similar $K_{(A)}$ values for Mg^{2+} in the presence of cAMP/cGMP were found. Classically, Mg^{2+} as cofactor maximally stimulated PDE from rat brain (53) and bovine retina (54,55) whereas Mn^{2+} and Co^{2+} only partially enhanced PDE. Our results indicate that the PDE1A from PM-BTSM showed kinetic parameters for the Mg^{2+} similar to others membrane bound PDEs (55).

PDE1s contain two Ca^{2+}/CaM-binding domains required for full activation. The CaM activation of the PDE1A from PM-BTSM was 2.2-fold (cAMP) and 1.8-times for cGMP. Moreover, this PDE1A displayed a high affinity for CaM $K_{(CaM)}$ which are close to reports of the recombinant PDE1A2 (45).

One valuable tool in this work was the inhibitory effect of vinpocetine. Thus, the vinpocetine displayed similar IC_{50} around 4.6–4.9 μM, independently of the cyclic nucleotides. Vinpocetine is a selective PDE1 inhibitor, being a specific pharmacological tool for PDE1 studies (51, 56, 57). Several PDE-1 displayed IC_{50} for vinpocetine (from 8 to 50 μM) (30). Interestingly, the IC_{50} values here described for vinpocetine are lower than the previously reported.

PDE1A family are involved in different biological processes (56,57) at the regulation of vascular smooth muscle contraction (58) and heart remodeling (59) and plays a role in function of the sperm (42,43). The function of the PDE1A from BTSM has to be correlated to the regulation of cyclic nucleotides levels in ASM. In this sense, our experimental findings supports a model, which is illustrated in Figure 7, where an original signal transducing cascade integrates by a M_2AChR, directly coupled to a PDE1A anchors at sarcolemma of ASM is proposed.

This PDE1A might participate in the regulation of cyclic nucleotides levels at the sub-plasmalemmal space in ASM. Thus, muscarinic antagonist drugs acting as ''inverse agonists'' on M_2AChR leading to the inhibition of this PDE1A increasing the cyclic nucleotide (cAMP, cGMP) content producing a profound relaxation of ASM, which is important in asthma. The relevant role of M_2AChR on the action of muscarinic antagonists is supported by the recent findings indicating that muscarinic antagonist drug as tiotropium bromide (which selectively antagonizes the M_3AChR subtype) in Ovalbumin-induced chronic asthma in mice (OVA) models, was able to inhibit the expression of the M_3AChR and increased the M_2AChR (60). It can be hypothesized that the muscarinic antagonist induces the M_2AChR expression and at the same time acting on M_2AChR can inhibit the PDE1A here described. Both synergistic effects can explain the powerful relaxation and beneficial therapeutic effects of these drugs on asthma patients.

This hypothesis has to be demonstrated in biomodels such as the OVA-induced asthma rats. In this sense, the future development of new drugs as compounds derivate from vinpocetine, that selective inhibit this novel PDE1A, which might be a promising pharmacological approach for the treatment of asthma or COPD.

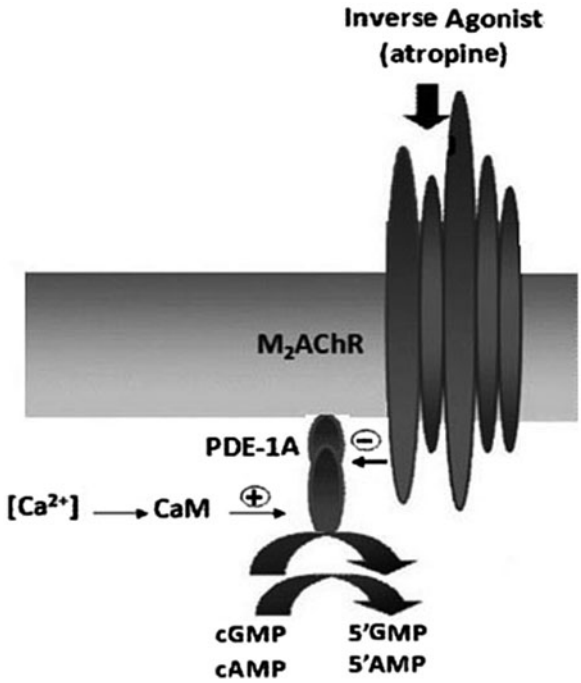

Figure 7. A model of a novel transducing cascade associated with muscarinic receptors (M2AChRs) and the PDE1A. This model of a signal transducing pathway of the airway smooth muscle (ASM) proposes that muscarinic agents (antagonists) acting as ''inverse agonists'' bind to the M2AChR located to ASM sarcolemma, which induces the inhibition of a plasma membrane-bound PDE1A, which is vinpocetine-inhibited and CaM stimulated enzyme. This last PDE1A inhibition can increase the cGMP/cAMP intracellular levels, inducing ASM relaxation.

Conclusions

The cyclic nucleotides (cAMP and cGMP) levels in bovine tracheal smooth muscle (BTSM) strips are modified in the presence of muscarinic antagonists. These effects are mimicked by vinpocetine, a PDE1 inhibitor, suggesting that a PDE1 is involved in the effects of muscarinic antagonists on BTSM strips. A PDE1 activity which was inhibited by vinpocetine, was located in enriched plasma membrane (PM) fractions from BSTM. These PM fractions exhibited only two muscarinic receptor sub-types identified as M_2 and M_3AChRs. This PDE1 activity in these PM fractions was strongly inhibited by muscarinic antagonists such as methoctramine relevant to an M_2AChR. The inhibition was less strong for 4-DAMP, related to M_3AChRs suggesting that an M_2AChR is involved in this biological effect. The membrane-bound PDE1 was removed from these PM fractions, using a hypotonic extraction and purified using two chromatography columns, an anion exchange (Q-sepharose) followed by a calmodulin-agarose (CaM) affinity column. The PDE1 activity was purified 38 times, yielding two bands in PAGE-SDS at 56 and 58 kDa. The 58 kDa band was identified as the PDE1A isoenzyme using Western blotting analysis. This isolated PDE1A exhibited inhibition by vinpocetine and activation by CaM.

This PDE1A activity assayed with [^{3}H]cGMP and [^{3}H]cAMP exhibited the following kinetic parameters: the

K_m for cAMP was 8.4 μM and for cGMP was 6.1 μM. The V_{max} ratio was 1.5 for cAMP/cGMP. Vinpocetine showed similar IC_{50} (4.9 and 4.6 μM) for cAMP and cGMP respectively. CaM stimulated this PDE1A activity exhibiting similar $K_{(CaM)}$, in the nM range for both cyclic nucleotides. The cofactor Mg^{2+} showed similar values for both cyclic nucleotides with a $K_{(A)}$ of 0.32 for cAMP and 0.24 mM for cGMP. The original finding is the identification of a vinpocetine-inhibited, atropine-inhibited and CaM-dependent plasma membrane-bound PDE1A, which is linked to M_2AChR possibly by direct interaction between M_2AChR intracellular loops with this PDE1A, which are support by the experimental data using muscarinic antagonists. This is the first report of the presence of a membrane-bound PDE1A at BTSM. Furthermore, a novel signal-transducing cascade with an M_2AChR linked to this PDE1A, at the sarcolemma of ASM is proposed (Figure 7). It is possible that this PDE1A participates in the regulation of cyclic nucleotide levels at the subplasmalemmal space in ASM. Muscarinic antagonist drugs, acting as ''inverse agonists'' on M_2AChR, leads to the inhibition of this PDE1A, increasing simultaneously the cyclic nucleotide content of both cAMP and cGMP, with the concomitant production of a profound ASM relaxation.

The future development of new drugs that selectively inhibit this novel PDE1A might be a promising pharmacological approach for the treatment of asthma or COPD.

Declaration of interest

The authors report no declarations of interest.This work was supported by grants from CDCH-UCV # PG 09-7772-2009/1(MJA) and CDCH-UCV # PG-09-7401-2008/2 (RGA) and CDCH-UCV # PI-09-7726.2009/2 (ILB). The authors thank Dr Coral Wynter for revision of the English version of this manuscript.

References

1. Van der Velden VH, Hulsmann AR. Autonomic innervation of human airways: structure, function, and pathophysiology in asthma. Neuroimmunomodulation 1999;6:145–59.
2. Belmonte KE. Cholinergic pathways in the lungs and anticholinergic therapy for chronic obstructive pulmonary disease. Proc Am Thor Soc 2005;2:297–304.
3. Gosens R, Zaagsma J, Meurs H, Halayko AJ. Muscarinic receptor signaling in the pathophysiology of asthma and COPD. Resp Res 2006;7:73–86.
4. Challiss RA, Adams D, Mistry R, Boyle JP. Second messenger and ionic modulation of agonist-stimulated phosphoinositide turnover in airway smooth muscle. Biochem Soc Trans 1993;21:1138–45.
5. Oldhman WM, Hamm HE. Heterotrimeric G protein activation by G-protein-coupled receptors. Nat Rev Mol Cell Biol 2008;9:60–71.
6. Kotenis E, Zeng FY, Wess J. Structure-function of muscarinic receptors and their associated G proteins. Life Sci 1999;64:335–62.
7. Maeda A, Kubo T, Mishina M, Numa S. Tissue distribution of mRNAs encoding muscarinic acetylcholine receptor subtypes. FEBS Lett 1998;239:339–42.
8. Eglen RM, Hedge SS, Watson N. Muscarinic receptor subtypes and smooth muscle function. Pharmacol Rev 1996;48:531–65.
9. Roffel AF, Elzinga CRS, Van Amsterdam RGM, et al. Muscarinic receptors in bovine tracheal smooth muscle: discrepancies between binding and function. Eur J Pharmacol 1988;153:73–82.
10. Misle AJ, Bécemberg IL, Alfonzo RG, Alfonzo MJ. Methoctramine binding sites sensitive to alkylation on muscarinic receptors from tracheal smooth muscle. Biochem Pharmacol 1994;48:191–5.
11. Hagiwara M, Endo T, Hidaka H. Effects of vinpocetine on cyclic nucleotide metabolism in vascular smooth muscle. Biochem Pharmacol 1984;33:453–7.
12. Guerra de González L, González de Alfonzo R, Lippo de Bécemberg I, Alfonzo MJ. Cyclic nucleotide-dependent phosphodiesterases (PDE1) inhibition by muscarinic antagonists in bovine tracheal smooth muscle. Biochem Pharmacol 2004;68:651–8.
13. Torphy TJ, Cieslinski LB. Characterization and selective inhibition of cyclic nucleotide phosphodiesterase isozymes in canine tracheal smooth muscle. Mol Pharmacol 1990;37:206–14.
14. Shahid M, Van Amsterdam R, De Boer J, et al. The presence of five cyclic nucleotide phosphodiesterase isoenzyme activities in bovine tracheal smooth muscle and functional effects of selective inhibitors. Br J Pharmacol 1991;104:471–7.
15. Beavo JA. Multiple isozymes of cyclic nucleotide phosphodiesterases. Adv Second Messengers Phosphoprot Res 1998;22:1–38.
16. Beavo JA. Cyclic nucleotide phosphodiesterases: functional implications of multiple isoforms. Physiol Rev 1995;75:725–48.
17. Sonnenburg WK, Seger D, Kwak KS, et al. Identification of inhibitory and calmodulin-binding domains of the PDE1A1 and PDE1A2 calmodulin-stimulated cyclic nucleotide phosphodiesterases. J Biol Chem 1995;270:30989–1000.
18. Guerra de González L, Misle A, Pacheco G, et al. Effects of 1H-[1, 2, 4]-oxadiazolo [4, 3-a] quinoxalin-1-one (ODQ) and N-omega (6)-nitro-L-arginine methyl ester (NAME) on cyclic GMP levels during muscarinic activation of tracheal smooth muscle. Biochem Pharmac 1999;58:563–9.
19. Lippo de Bécemberg I, Correa de Adjounian MF, et al. G-protein-sensitive guanylyl cyclase activity associated with plasma membranes. Arch Biochem Biophys 1995;324:209–15.
20. González de Alfonzo R, Bécemberg IL, Alfonzo MJ. A Ca^{2+}/CaM dependent protein kinase associated with Ca^{2+} transport in sarco(endo)plasmic vesicles from tracheal smooth muscle. Life Sci 1996;58:18–24.
21. Gillespie PG, Beavo JA. Characterization of a bovine cone photoreceptor phosphodiesterase purified by cyclic GMP-sepharose chromatography. J Biol Chem 1988;263:8133–41.
22. Sharma R, Wang T, Wirch E, Wang J. Purification and properties of bovine brain calmodulin-dependent cyclic nucleotide phosphodiesterase. J Biol Chem 1980;255:5916–23.
23. Benaim G, Zurini M, Carafoli E. Different conformational status of the purified Ca^{2+}-ATPase of the erythrocyte plasma membrane revealed by controlled trypsin proteolysis. J Biol Chem 1984;259:8471–7.
24. Laemmli UK. Cleavage of structural proteins during the assembly of the head of bacteriophage T4. Nature Lond) 1970;227:680–85.
25. Towbin H, Staehelin T, Gordon J. Electrophoretic transfer of proteins from polyacrylamide gels to nitrocellulose sheets: procedure and some applications. Proc Natl Acad Sci USA) 1979;76:4350–4.
26. Bensadoum A, Weinstein D. Assay of proteins in the presence of interfering materials. Anal Biochem 1976;70:241–50.
27. Perez JF, Sanderson MJ. The frequency of calcium oscillations induced by 5-HT, ACH, and KCl determine the contraction of smooth muscle cells of intrapulmonary bronchioles. J Gen Physiol 2005;125:535–53.
28. Pacheco G, Bécemberg IL, Alfonzo RG, Alfonzo MJ. Biochemical characterization of a V-ATPase of tracheal smooth muscle plasma membranas. Biochim Biophys Acta 1996;1282:182–92.
29. Kamm K, Stull J. Regulation of smooth muscle contractile elements by second messengers. Ann Rev Physiol 1989;51:299–313.
30. Beavo J, Houslay MD. Cyclic nucleotide phosphodiesterases: structure, function, regulation, and drug action. Chichester, United Kingdom: John Wiley & Sons; 1990.
31. Michel AD, Whiting RL. Methoctramine reveals heterogeneity of M2 muscarinic receptors in longitudinal ileal smooth muscle membranes. Eur J Pharmacol 1988;145:305–11.
32. Michel AD, Stefanich E, Whiting RL. Direct labeling of rat M3-muscarinic receptors by [^{3}H]-4DAMP. Eur J Pharmacol 1989;166:459–66.
33. Sankary RM, Jones CA, Madison JM, Brown JK. Muscarinic cholinergic inhibition of cyclic AMP accumulation in airway smooth muscle. Role of a pertussis toxin-sensitive protein. Am Rev Respir Dis 1988;138:145–50.
34. Zhou XB, Wulfsen I, Lutz S, et al. M2 muscarinic receptors induce airway smooth muscle activation via a dual, G βγ-mediated Inhibition of large conductance Ca^{2+}-activated K channel activity. J Biol Chem 2008;283:21036–44.

35. Nakahara T, Yunoki M, Mitani A, et al. Stimulation of muscarinic M_2 receptors inhibits atrial natriuretic peptide-mediated relaxation in bovine tracheal smooth muscle. Naunyn Schmiedebergs Arch Pharmacol 2002;366:376–9.
36. Alfonzo MJ, Placeres-Uray F, Hassan-Soto W, et al. Two guanylylcyclases regulated the muscarinic activation of airway smooth muscle. In: Sugi H, ed. Current basic and pathological approaches to the function of muscle cells and tissues-from molecules to humans. Croatia: InTech; 2012:113–32.
37. Uray FP, de Alfonzo RG, de Becemberg IL, Alfonzo MJ. Muscarinic agonists acting through M2 acetylcholine receptors stimulate the migration of an NO-sensitive guanylyl cyclase to the plasma membrane of bovine tracheal smooth muscle. J Recept Signal Transduct Res 2010;30:10–23.
38. Kan W, Adjobo-Hermans M, Burroughs M, et al. M3 muscarinic receptor interaction with phospholipase Cβ3 determines its signaling efficiency. J Biol Chem 2014;289:11206–18.
39. Artemyev NO, Surendran R, Lee JC, Hamm HE. Subunit structure of rod cGMP-phosphodiesterase. J Biol Chem 1966;271:25382–88.
40. Baehr W, Devlin MJ, Applebury ML. Isolation and characterization of cGMP phosphodiesterase from bovine rod outer segments. J Biol Chem 1979;254:11669–77.
41. Anant JS, Ong OC, Xie HY, et al. In vivo differential prenylation of retinal cyclic GMP phosphodiesterase catalytic subunits. J Biol Chem 1992;267:687–90.
42. Chaudhry PS, Casillas ER. Calmodulin-stimulated cyclic nucleotide phosphodiesterases in plasma membranes of bovine epididymal spermatozoa. Arch Biochem Biophys 1988;262:439–44.
43. Lefiévre L, Lamirande E, Gagnon C. Presence of cyclic nucleotide phosphodiesterases PDE1A, existing as a stable complex with calmodulin, and PDE3A in human spermatozoa. Biol Reprod 2002; 67:423–30.
44. Snyder PB, Florio VA, Ferguson K, Loughney K. Isolation, expression and analysis of splice variants of a human Ca2+/calmodulin stimulated phosphodiesterase (PDE1A). Cell Signal 1999;11:535–44.
45. Rybalkin S, Yan C, Bornfeldt K, Beavo JA. Cyclic GMP phosphodiesterases and regulation of smooth muscle function. Circ Res 2003;93:280–91.
46. Vasta V, Sonnenburg WK, Yan C, et al. Identification of a new variant of PDE1A calmodulin-stimulated cyclic nucleotide phosphodiesterase expressed in mouse sperm. Biol Reprod 2005; 73:598–609.
47. Michibata H, Yanaka N, Kanoh Y, Okumura K, Omori K. Human Ca^{2+}/calmodulin-dependent phosphodiesterase PDE1A: novel splice variants, their specific expression, genomic organization, and chromosomal localization. Biochim Biophys Acta 2001;1517: 278–87.
48. Fidock M, Millar M, Lanfear J. Isolation and differential tissue distribution of two human cDNAs encoding PDE-1 splice variants. Cell Signal 2002;14:53–60.
49. Omori K, Kotera J. Overview of PDEs and their regulation. Circ Res 2007;100:309–27.
50. Bender A, Beavo JA. Cyclic nucleotide phosphodiesterases: molecular regulation to clinical use. Pharmacol Rev 2006;58: 488–520.
51. Keravis T, Lugnier C. Cyclic nucleotide phosphodiesterase PDE) isozymes as targets of the intracellular signaling network: benefits of PDE inhibitors in various diseases and perspectives for future therapeutic developments. British Pharmacol 2012;165:1288–1305.
52. Wasco WM, Kincaid RL, Orr GA. Identification and characterization of calmodulin-binding proteins in mammalian sperm flagella. J Biol Chem 1989;264:5104–11.
53. Cheung WY. Properties of 3',5'-nucleotide phosphodiesterase from rat brain. Biochemistry 1967;6:1079–87.
54. Chader G, Johnson M, Fletcher R, Bensinger R. Cyclic nucleotide phosphodiesterase of the bovine retina: activity, subcellular distribution and kinetics parameters. J Neurochem 1974;22:93–9.
55. Srivastava D, Fox DA, Hurwitz L. Effects of magnesium on cyclic GMP hydrolysis by the bovine retinal rod cyclic GMP phosphodiesterase. Biochem J 1995;308:653–8.
56. Lugnier C. Cyclic nucleotide phosphodiesterase (PDE) superfamily: a new target for the development of specific therapeutic agents. Pharmacol Therap 2006;109:266–398.
57. Jeon YH, Heo YS, Kim CM, et al. Phosphodiesterase: overview of protein structures, potential therapeutic applications and recent progress in drug development. Cell Mol Life Sci 2005;62: 1198–220.
58. Chain S, Yan C. PDE1 isozymes, key regulators of pathological vascular remodeling. Curr Opin Pharmacol 2011;11:720–4.
59. Miller C, Cai Y, Oikawa M, et al. Cyclic nucleotide phosphodiesterase 1A: a key regulator of cardiac fibroblast activation and extracellular matrix remodeling in the heart. Basic Res Cardiol 2011;106:1023–39.
60. Kang JY, Rhee CK, Kim JS, et al. Effect of tiotropium bromide on airway remodeling in a chronic asthma model. Ann Allergy Asthma Immunol 2012;109:29–35.